



Dedicated to innovation in aerospace

NLR-TP-2020-114 | May 2020

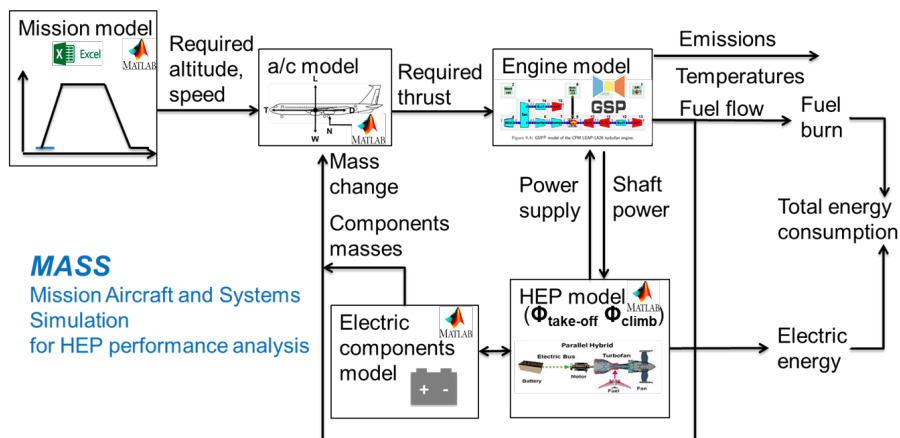
Energy Optimization of Single Aisle Aircraft with Hybrid Electric Propulsion

CUSTOMER: NLR



NLR – Royal Netherlands Aerospace Centre

Energy Optimization of Single Aisle Aircraft with Hybrid Electric Propulsion



Problem area

Air travel has increased considerably over the past decades and it is expected to double in the next two decades. The combination of the rising demand for air transport and the need to decrease environmental impact of aircraft (exploitation of non-renewable fossil fuels, emission of greenhouse gasses and particles, and noise) put a strong challenge on the aircraft industry to come up with innovative technologies.

In the automotive industry hybrid and fully electric cars have been developed in order to reduce environmental impact. In the aircraft industry, fully electric propulsion has been introduced for light aircraft so far. The low power-to-weight and energy-to-weight ratios of present state-of-the-art electric components, in particular of batteries, hold back the development of fully electric commercial passenger aircraft in the short term. Nevertheless, Hybrid Electric Propulsion (HEP) systems may bring solutions sooner by combining state of the art turbofan engines with innovative electric systems.

There is a strong interest to analyze and optimize the potential fuel, energy and emission reductions of HEP for single aisle passenger aircraft.

REPORT NUMBER
NLR-TP-2020-114

AUTHOR(S)
W.F. Lammen
W.J. Vankan

REPORT CLASSIFICATION
UNCLASSIFIED

DATE
May 2020

KNOWLEDGE AREA(S)
Computational Mechanics and Simulation Technology
Aerospace Collaborative Engineering and Design

DESCRIPTOR(S)
hybrid electric propulsion
MASS
single aisle aircraft
A320
emissions

Description of work

In the context of the EU Clean Sky 2 project NOVAIR a study was performed that focusses on a parallel HEP architecture 'retrofitted' to an Airbus A320neo reference aircraft. To support the study a parametric system model and tool chain was developed, called MASS: Mission, Aircraft and Systems Simulation for HEP performance analysis and system optimization.

Two levels of aircraft and electric component technology were evaluated to assess and optimize the performance of HEP: the technology level of "today" and an estimated technology level for 2035 including a projection of the reference aircraft to entry into service (EIS) in 2035. In both cases a short range mission (1500 km) with 150 passengers was applied.

Results and conclusions

The resulting tool chain - MASS - simulates the performance of a specified aircraft configuration, including engines and electric systems, for a given mission. The fuel flow and electric power are calculated as function of time in order to predict the total energy consumption. Furthermore the engine emissions are calculated.

When assuming the technology level of "today" the application of parallel HEP does not show any benefit in terms of fuel or energy reduction. When assuming an estimated technology level for 2035 – including a reference aircraft with EIS in 2035 - reductions of fuel and total energy consumption up to 7% and 5 % respectively can be achieved when applying parallel HEP. When taking into account emissions as well, a compromised optimum was found, which results in 6% fuel reduction, 2% energy reduction and 1.5% NOx reduction.

Additional trend analysis with varying specific energy and specific power assumptions of the electric components shows that the impact of these variations on the minimized energy consumption is small.

Applicability

Besides for the A320neo, MASS can be used for performance analysis of any aircraft mission combination with HEP. The efficient simulation models can be used for sensitivity analysis and optimization studies supporting the conceptual and multidisciplinary design of aircraft with HEP, or for retrofit studies.

GENERAL NOTE

This report is based on a presentation held at the AIAA SciTech Forum, Orlando FL, 07/01/2020.

NLR

Anthony Fokkerweg 2

1059 CM Amsterdam, The Netherlands

p) +31 88 511 3113

e) info@nlr.nl i) www.nlr.nl



Dedicated to innovation in aerospace

NLR-TP-2020-114 | May 2020

Energy Optimization of Single Aisle Aircraft with Hybrid Electric Propulsion

CUSTOMER: NLR

AUTHOR(S):

W.F. Lammen

NLR

W.J. Vankan

NLR

This report is based on a presentation held at the AIAA SciTech Forum, Orlando FL, 07/01/2020.

The contents of this report may be cited on condition that full credit is given to NLR and the authors.

This publication has been refereed by the Advisory Committee AEROSPACE VEHICLES (AV).

CUSTOMER	NLR
CONTRACT NUMBER	CS2-LPA-GAM-2018/2019-01
OWNER	NLR
DIVISION NLR	Aerospace Vehicles
DISTRIBUTION	Unlimited
CLASSIFICATION OF TITLE	UNCLASSIFIED

APPROVED BY:		Date
AUTHOR	W.F. Lammen	31-03-2020
REVIEWER	H. Jentink	31-03-2020
MANAGING DEPARTMENT	A.A. ten Dam	13-05-2020

Energy Optimization of Single Aisle Aircraft with Hybrid Electric Propulsion

Wim Lammen¹ and Jos Vankan²

NLR- Royal Netherlands Aerospace Centre, P.O. Box 90502, 1006 BM Amsterdam, The Netherlands

This study investigates the reduction of aircraft fuel and energy consumption, and emissions through the introduction of hybrid electric propulsion (HEP) on an Airbus A320 type aircraft. The following electric systems are considered: electric motors, batteries and power electronics. This study focusses on the parallel HEP architecture. The power and energy sizing of the electric components, as well as their mass effects on overall aircraft mission performance are evaluated by integrated system modelling of the aircraft, turbofan and the considered electric components. Variations of aircraft and electric component technology levels are evaluated to assess and optimize the performance of HEP. When assuming the technology level of “today” the application of parallel HEP does not show any benefit in terms of fuel or energy reduction. When assuming an estimated technology level for 2035 – including a reference aircraft with entry into service (EIS) in 2035 - reductions of fuel and total energy consumption up to 7% and 5 % respectively can be achieved when applying parallel HEP. Furthermore it is found that the minimizations of fuel burn, energy consumption, and NOx emission counteract each other. In the 2035 scenario a compromised optimum was found, which results in 6% fuel reduction, 2% energy reduction and 1.5% NOx reduction. Additional trend analysis with varying specific energy and specific power assumptions of the electric components shows that the impact of these variations on the minimized energy consumption is small.

I. Introduction

Air travel has increased considerably over the past decades and it is expected to double in the next two decades [1]. The combination of the rising demand for air transport and the need to decrease environmental impact of aircraft (a/c) put a strong challenge on the aircraft industry to come up with innovative technologies [2].

In the automotive industry hybrid and fully electric cars have been developed in order to reduce environmental impact. In the aircraft industry, fully electric propulsion has been introduced for light aircraft so far [3]. The low power-to-weight and energy-to-weight ratios of present state-of-the-art electric components, in particular of batteries, hold back the development of fully electric commercial passenger aircraft in the short term. Nevertheless, Hybrid Electric Propulsion (HEP) systems may bring solutions sooner by combining state of the art turbofan engines with innovative electric systems.

Various aircraft concepts involving several types of HEP were recently investigated [3], [4]. The different types of HEP can be divided into serial and parallel architectures. In serial architectures mechanical power is extracted from a thermal engine, converted to electric power and transferred to electrically driven propulsors. In parallel architectures electric power is extracted from batteries and converted to mechanical power by electric motors. This mechanical power is added to the thermal engine’s mechanical power at the propulsor³, see Fig. 1.

¹ R&D Engineer Modelling and Simulation, Collaborative Engineering Systems dept.

² Principal Scientist Multidisciplinary Design and Optimization, Collaborative Engineering Systems dept.

³ Distributed electrically driven propulsors that run in parallel to the thermal engine, are of interest too but are not considered in this paper.

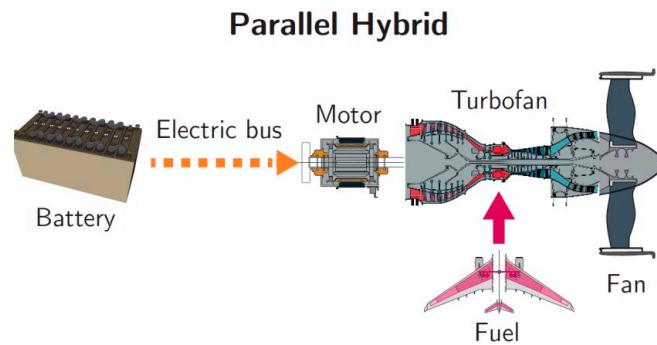


Fig. 1 Schematic of the parallel HEP architecture as considered in this study (adapted from Ref.[5]).

Another clear trend in aircraft design is the electrification of non-propulsive systems. Examples of such “More Electric Aircraft” (MEA) are the Boeing 787 and Airbus A350. These aircraft feature advanced electrically powered systems instead of their conventional hydraulic and pneumatic counterparts. Such more electric system architectures also have potential to increase energetic efficiency on aircraft level and thus contribute to aircraft fuel and energy reduction.

In the NOVAIR project – carried out by TU Delft (Delft University of Technology) and NLR as part of the EU Clean Sky 2 program Large Passenger Aircraft (LPA) [6] – investigations on HEP for single aisle LPA are performed [7],[8]. The study presented here focusses on a parallel HEP architecture (see Fig. 1), retro-fitted to an Airbus A320neo reference aircraft. Previous results from these investigations were recently published [9], [10], [11], and [12]. The investigations reported in these papers concern several additional system and mission variations that impact the energetic performance of the A320neo with HEP, such as

- the downscaling of the turbofan engine [9], [10], [11], and [12];
- the conversion to an electrical architecture of the non-propulsive power systems (the MEA approach) [10], [11], and [12];
- the application of electric taxiing [9], [10], and [11];
- the implementation of a fuel cell system and the installation of photovoltaic panels on the top surfaces of the aircraft [10] and [11];
- mission variations such as payload, range and cruise speed to analyze the effects on fuel and energetic performance [12].

All of these HEP investigations were performed for short-range missions (1000 km [9], [10] or 1500km [11], [12]). The largest effects on the energetic and fuel performance were found to be caused by the downscaling of the turbofan engine and by applying the MEA approach (see Ref. [11]). The energetic and fuel performances also depend on the assumed technology level of the involved electric components. A literature study was performed (see Ref. [10]) with respect to expected specific energy, specific power and efficiency values of the electric components (i.e. batteries, motors and inverters) in the future. This resulted in “near future” (2020 – 2040) and “far future” (after 2040) technology scenarios. The analysis was performed by comparing the system modifications in combination with assumed HEP technology levels against the A320neo reference aircraft.

In this paper technology predictions are made for an aircraft with Entry-Into-Service (EIS) in 2035. To focus the analysis specifically on the impact of HEP we compare the a/c with HEP to a reference a/c also with EIS in 2035 but without HEP. The system modifications described above are left out, except the downscaling of the turbofan engine. Downscaling the engine is essential for achieving energetic benefits with parallel HEP: assisting the engine in peak power phases (i.e. take-off and climb) by additional power from electric motors allows the engine to be downscaled which results in a lower engine weight and better performance during the cruise phase [11], [12]. In addition to the performance analyses in terms of fuel and total energy consumption, aircraft emissions are considered as well.

Furthermore the current A320neo reference a/c is compared to a version with parallel HEP using the current state of the art electric component technology. In this paper this comparison is referred to as the “2015 scenario”, taking into account technology that is available since 2015 and the A320neo, which entered into service in January 2016.

In the following sections, first the methodology including the involved models and the implemented analysis tool chain is described. Second the simulation assumptions are presented and discussed including the modification of the A320neo to be used as reference a/c with EIS in 2035. Then the simulation and optimization results are presented for different technology level scenarios and variations of electric component specific power and energy. Finally, conclusions and perspectives are given.

II. Modelling & Simulation approach

A. Parametric analysis tool chain “MASS”

The analysis of the performance of the HEP a/c in comparison to the reference a/c is carried out by modelling and simulation. A dedicated tool chain of parametric models for HEP performance analysis has been developed in MATLAB⁴ (see Fig. 2). This tool chain (MASS: Mission, Aircraft and Systems Simulation) simulates the performance of a specified aircraft configuration, including engines and electric systems, for a given mission. The fuel flow and electric power are calculated as function of mission time in order to predict the total trip energy consumption. Furthermore the engine emissions are calculated.

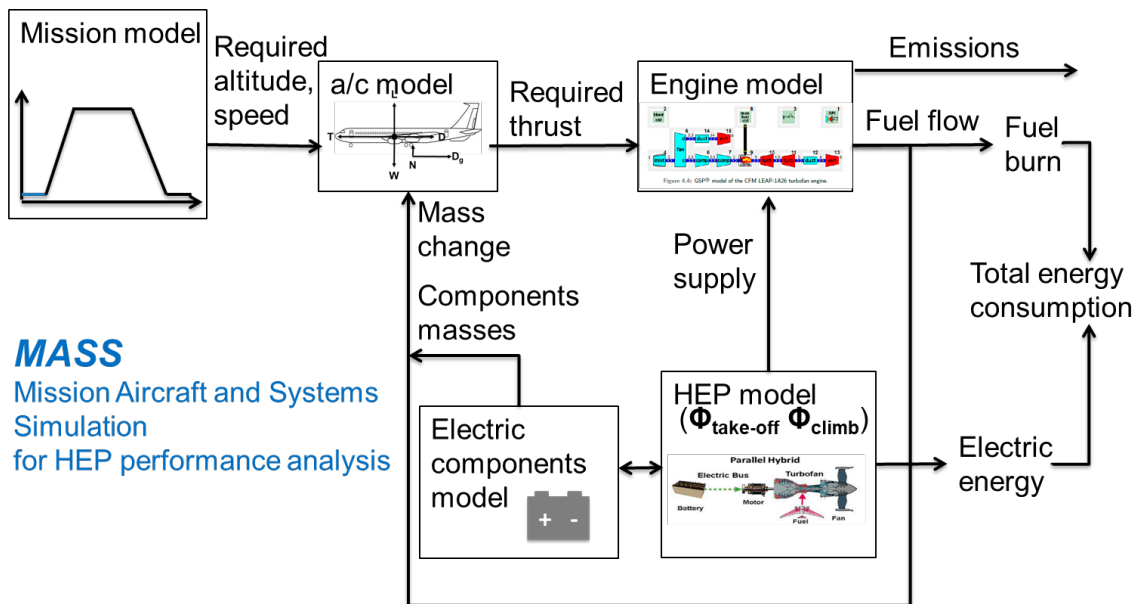


Fig. 2 “MASS” tool chain for HEP performance analysis.

In the following subsections the components of MASS are described in the context of the A320neo reference a/c. Other aircraft types can be simulated as well, but are not considered in this paper.

1. Mission model

The mission model reads an Excel table that contains the a/c altitude, speed, and flap and landing gear settings as a function of horizontal distance. An arbitrary mission can be defined that suitable for the specified aircraft. In this case an Airbus A320 mission of 800 NM (1500 km) with climb of 250 and 275 knots Indicated Air Speed (KIAS) and 0.78 Mach cruise was derived from Ref.[13]. The mission model calculates the flight path variables (altitude, distance, speeds, flight path angle etc.) as function of flight time, by means of linear interpolation. The flight time is calculated from the distance travelled at the interpolated speed. Fig. 3 shows the 800 NM mission - considered in this paper - as calculated by the mission model.

⁴ <http://www.mathworks.com>

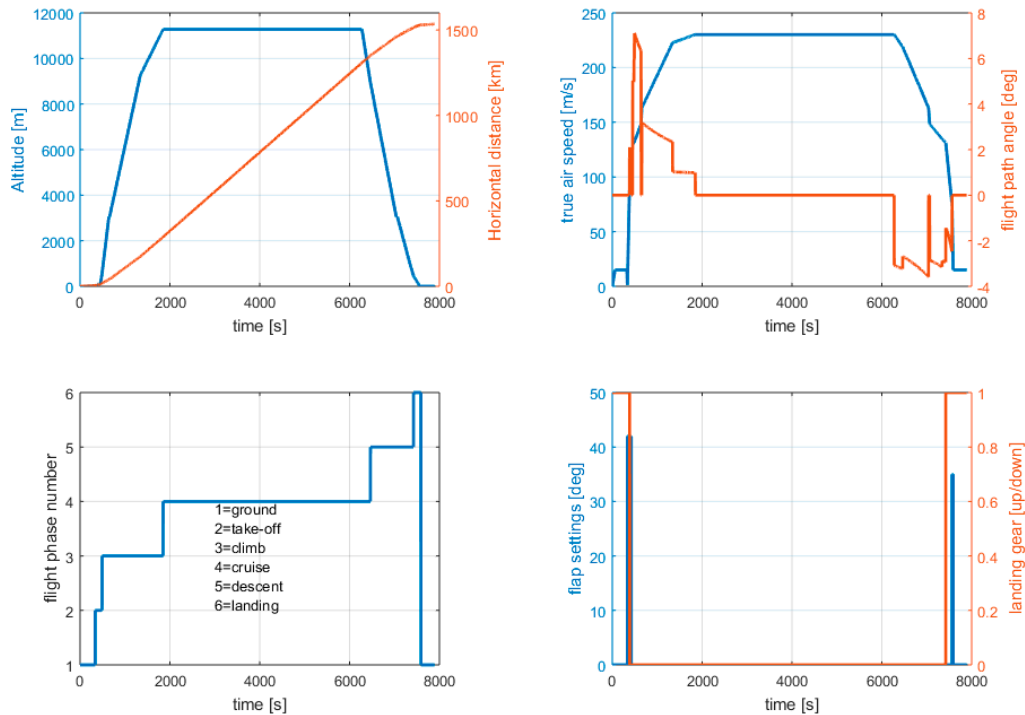


Fig. 3 Output of the mission model for the A320 reference mission derived using Ref.[13].

2. Aircraft model

The aircraft model takes as input the flight path variables from the mission model in combination with a/c specific parameters (such as the a/c mass, and lift and drag coefficients as function of flap and gear settings and Mach number) and calculates the required thrust as function of time. The model is based on a so-called “point mass” representation of the aircraft, see Fig. 4. Both flight and on-ground behavior have been modelled, taking into account normal forces and rolling friction as well as dependency of the aerodynamic coefficients on flap and gear settings and Mach number.

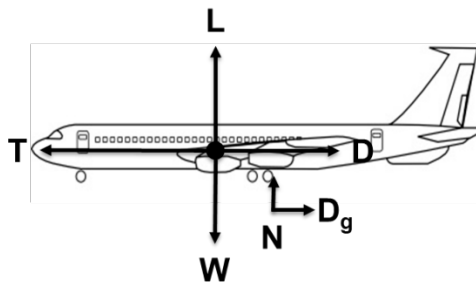


Fig. 4 Illustration⁵ of the forces in the basic aerodynamic “point mass” model, with forces: D drag, D_g ground friction, N normal, L lift, W weight and T thrust.

Only forward motion and flight path angle are included in the present study’s flight mission; turns and maneuvers and roll and yaw rotations are not considered. The equations below detail the calculation process of the thrust variable F_N . SI-units are applicable. Changes in flight path angle γ are approximated by (piecewise) circular motion (see Eq. 6).

$$F_N = m \cdot \dot{v} + D + D_{ground} + m \cdot g \cdot \sin \gamma \quad (1)$$

$$\sin \gamma = \frac{\dot{h}}{v} \quad (2)$$

⁵ Picture adapted from <https://simple-drawing.com/img/plane-outline-drawing-22.html>

Where v is true air speed (TAS), h is altitude, g is gravity, L is lift force and m is aircraft mass. The drag forces D and D_{ground} are calculated by

$$D = C_D \cdot \frac{1}{2} \rho \cdot v^2 \cdot S_w \quad (3)$$

$$D_{ground} = \mu \cdot N \quad (4)$$

Where ρ is air density, S_w is total wing area, N is normal force ($N=0$ in the air) and μ is ground rolling friction coefficient [13].

$$N = m \cdot g - \frac{1}{2} \rho \cdot v^2 \cdot S_w \cdot C_{L_0} \quad (5)$$

$$L = m \cdot v \cdot \dot{\gamma} + (m \cdot g - N) \cdot \cos \gamma \quad (6)$$

$$C_L = \frac{L}{\frac{1}{2} \rho \cdot v^2 \cdot S_w} \quad (7)$$

$$C_D = C_{D_0} + k C_L^2 + \Delta C_{D_{flaps}} + \Delta C_{D_{gear}} + \Delta C_{D_{Mach}} \quad (8)$$

C_L and C_D are the aerodynamic lift and drag coefficients, C_{L_0} the lift coefficient at zero angle of attack and C_{D_0} the zero-lift drag coefficient, ΔC_{D_x} the drag coefficients dependent on flaps, gear and Mach number respectively, and k the induced drag coefficient. The time derivatives \dot{v} , \dot{h} , and $\dot{\gamma}$ are approximated numerically.

The main model parameters used to specify the A320neo a/c (A320-251N [14]) that is considered in this study are given in Table 1 below. The a/c thrust that is needed for the mission illustrated in Fig. 3 is depicted in Fig. 5.

Table 1 The main parameter settings for the reference aircraft [14][15].

A320neo property	Value
Max. take-off mass, kg	73,500
Operating Empty mass, kg	45,700
Max. landing mass, kg	66,300
Wing area, m ²	122
Wing span, m	35.8

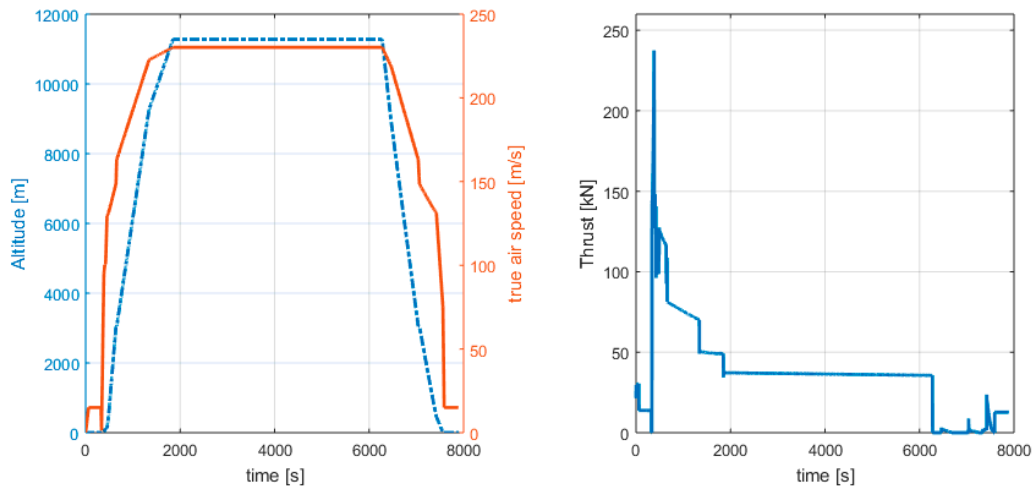


Fig. 5 Altitude and speed as function of time (left) and corresponding required thrust (right) calculated by the a/c model for the A320neo reference a/c.

3. Engine model

The aircraft model provides the required thrust and the mission model provides the ambient conditions to the engine model. This engine model was created using NLR's Gas-Turbine Simulation Program (GSP)⁶, which is based on thermodynamic modelling of mass- and energy-balances of the main engine components (compressors, combustor, turbines, fan etc., see Fig. 6). The GSP model allows simulating effects on fuel consumption and emissions of the common primary aircraft operational parameters like thrust, speed, altitude and payload. But also secondary parameters like bleed offtakes from the various compressor stages or mechanical shaft power offtakes from the Low Pressure Turbine (LPT) or High Pressure Turbine (HPT) shafts are considered. Vice versa, the GSP model also allows simulating the supply of mechanical power to the LPT or HPT shafts, and the effects of that on fuel flow in the engine. That is exactly what is of interest in parallel HEP system studies: the effects on the turbofan fuel flow of mechanic power supply through electric motor drives to the LPT or HPT shafts.

Moreover, in GSP one can model scaled versions of the original turbofan engine as well, which is essential in combination with parallel HEP, see section I. In the present study [9] the downscaling is performed by changing the engine diameter D and reducing the design inlet mass flow proportional to the square of the reduction D , according to Eq. (9).

$$\frac{\dot{m} \cdot \sqrt{\theta}}{D^2 \cdot \delta} = \text{constant} \quad (9)$$

Here δ and θ represent the dimensionless pressure and temperature correction parameters, respectively [9], that normalize the mass flow to the corrected mass flow⁷.

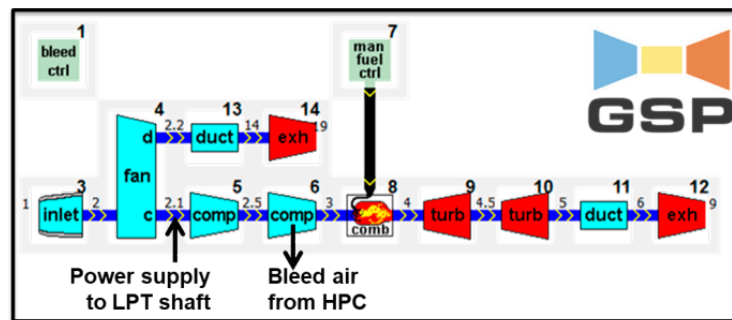


Fig. 6 Turbofan engine model in NLR's software tool GSP⁶

In the present study an engine model of the CFM-LEAP-1a26 [16], which is one of the engine options on the A320neo aircraft, has been implemented in the GSP software. The main specifications of the CFM-LEAP engine as incorporated in the GSP model are given in Table 2 below. Typical secondary offtake values in terms of bleed mass flow as a fraction of the engine total mass flow, and shaft power take-off (PTO) are listed in Table 3. These values were derived using Ref.[17], Ref.[18] and Ref.[19].

Besides calculation of the fuel consumption also specific engine emissions are predicted in terms of oxides of nitrogen (NO and NO₂, collectively referred to as NO_x), carbon monoxide (CO), and unburned hydrocarbons (UHC, usually expressed as equivalent methane)⁸. The emissions are calculated by interpolation of the emission indices, provided by the ICAO Aircraft Engine Emissions Databank [20]. This database contains emission measurement results for a variety of a/c engines, expressed in grams of emitted substance per kilogram of burned fuel. The corresponding emission indices for the CFM-LEAP-1a26 are given in Table 4. Carbon dioxide (CO₂) and water vapor (H₂O) emissions are not addressed in this table as they are considered directly proportional to the burned fuel [9].

⁶ <http://www.gspteam.com>

⁷ https://en.wikipedia.org/wiki/Corrected_flow

⁸ Other emitted substances such as soot/particulate matter or sulfur oxides (SO_x) are of interest too, but are not considered in this paper.

Table 2 Main specifications of the CFM-LEAP engine as incorporated in the engine model [16].

CFM-LEAP-1A26 property	Value
Engine mass (wet), kg	2990
Max. take-off thrust , kN	120.6
Max. continuous thrust, kN	118.7
Overall pressure ratio	40
LP rotor speed (N1 100%), RPM	3856
HP rotor speed (N2 100%), RPM	16645
Number of compressor stages (fan/LPC/HPC)	1/3/10
Number of turbine stages (HPT/LPT)	2/7

Table 3 Bleed and shaft off take values for the reference aircraft mission [17],[18],[19].

Flight phase	Customer Bleed fraction	PTO, kW per engine
Taxi	0.1	35
Take-off	0.03	37
Climb	0.05	42
Cruise	0.06	40
Descent	0.1	35
Landing	0.04	35

Table 4 Emission indices in g per kg fuel for the CFM-LEAP-1a26 [20].

Mode	Power setting, %	UHC, g/kg	CO, g/kg	NOx, g/kg
take-off	100	0.02	0.24	30.8
climb	85	0.02	0.26	13.38
approach	30	0.04	2.65	8.75
idle	7	0.29	21.63	4.61

In order to achieve an efficient coupling with the aircraft model a surrogate model has been derived from the GSP model of the CFM-LEAP-1a26. A data set of 5300 steady state GSP results with 6 varied inputs was fitted using an artificial neural network algorithm. The resulting engine surrogate model (ESM) predicts, besides the fuel flow and NO_x, CO and UHC emissions, also the LPT shaft power (in kW) and HPT total inlet temperature (TT4 in K). The inputs for the ESM are altitude (in m), airspeed (in Mach), required net thrust (in kN), customer bleed flow fraction (in %), LPT shaft offtake (in kW) and engine downscaling diameter ratio (in %). The outputs have a relative prediction error between 1 and 2 % in comparison to the GSP data set. The predicted fuel flow is used to calculate the total fuel burn (in kg) and the momentary fuel mass, which is fed back into the aircraft model after each time step of the mission evaluation time integration. The output LPT shaft power is used to predict the shaft power needed to provide the required thrust, which information is needed to apply parallel HEP. The HPT total inlet temperature (TT4) can be used to monitor the thermal load of the engine. For example in relation to engine downscaling TT4 can be used as a constraint to make sure that the engine load does not become too high. More information on the engine downscaling approach can be found in Ref.[9] and Ref.[10]. The outputs of the ESM in context of the CFM-LEAP-1a26 for the mission illustrated above (see Fig. 3 and Fig. 5) are shown in Fig. 7.

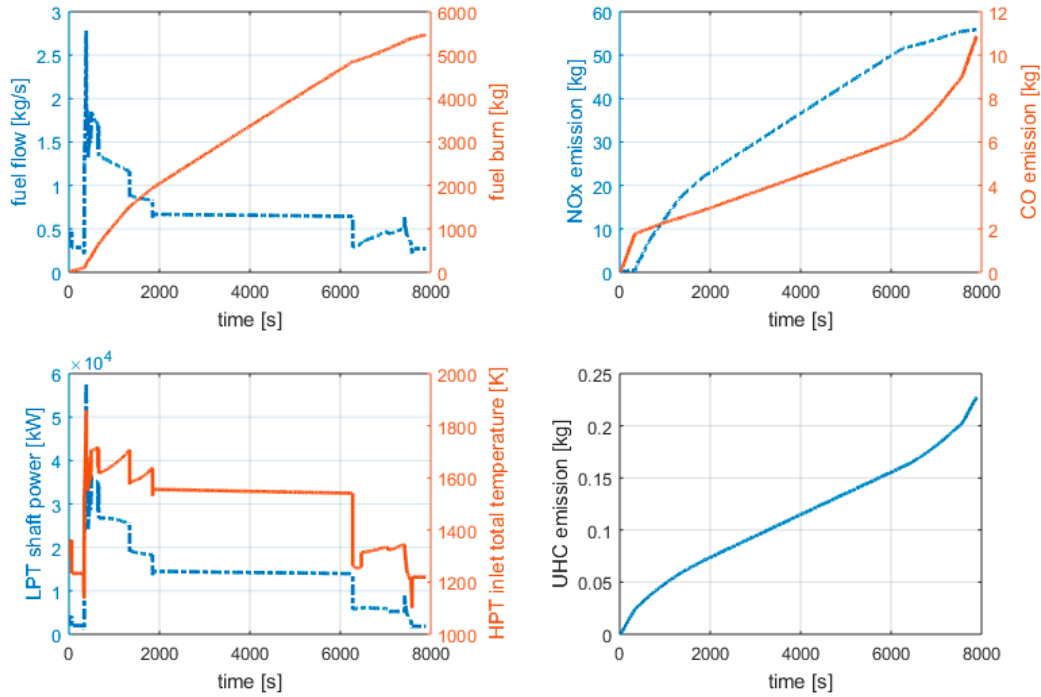


Fig. 7 Outputs of the ESM of the CFM-LEAP-1A26 as function of time.

4. HEP and electric components model

A standard analysis with MASS consists of a mission simulation with the reference aircraft followed by a repeat of this simulation with the electrified aircraft: the hybrid run. For this part the *HEP model* was created. To control the HEP and electric components model the *power split* ratio φ is defined:

$$\varphi = \frac{P_{EM}}{P_{tot}} \quad (10)$$

With P_{EM} the power supplied by the electric motors to the engine shafts and P_{tot} the total engine shaft power (required by the reference a/c and mission). In the current study parallel HEP is applied during take-off and climb only. $\varphi = 0$ during the other flight phases, see Fig. 8.

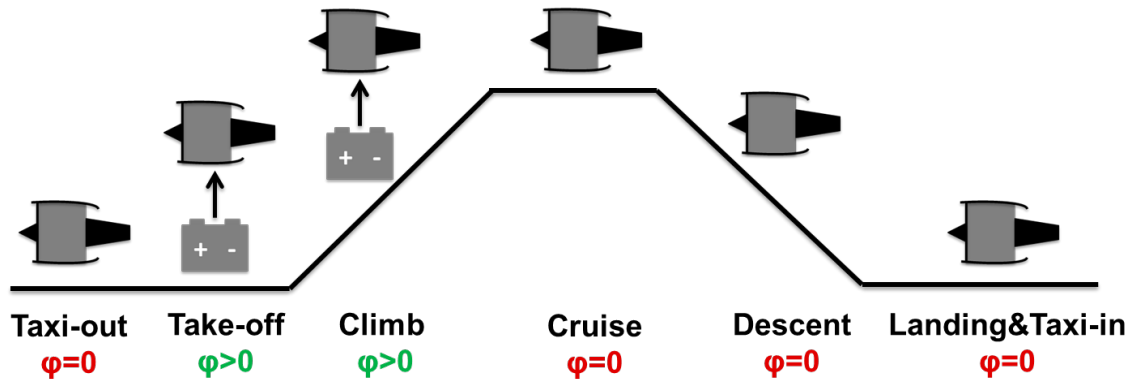


Fig. 8 Power split schedule per flight phase.

The HEP model connects with submodels of the involved electric components. The electric components considered in this study are the electric motors that drive the LPT shafts⁹, power electronics (mainly inverters), electric power cables, batteries and optionally fuel cells and solar cells. The electric components are included as mass contributions in the overall system model. As such, the electric components are included as basic “black box” models, see Fig. 9, with electric power and/or energy demands as inputs, and predicted component mass as output.

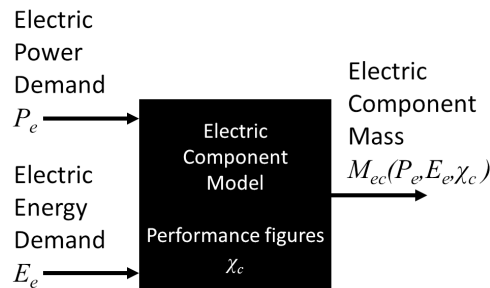


Fig. 9 The electric components are included as basic “black box” models.

For electric motors and power electronics the mass is determined from the required *maximum power level* of the electric system and from the specific power and the energetic efficiency of these components. For batteries the mass is determined from the required *maximum energy consumption* of the electric system and from the specific energy of the batteries. Of course, also the required *maximum power level* and the specific power of the batteries is important, but in this study the *maximum energy consumption* dominates the sizing process for the batteries. Furthermore the battery energy efficiency and minimum state of charge (SoC) are taken into account in the sizing process. The batteries’ energetic efficiency accounts for the recharge energy losses and therefore is only used for the total energy calculation, not for the battery mass calculation. Energetic efficiencies of electric power cables are also accounted for. The mass of the electric cables is not accounted for separately but is included in the power electronics mass.

The resulting total (electric) system mass is added to the total a/c mass and provided to the aircraft model during the hybrid run. In addition, the power supplied by the electric motors as function of time and power split ϕ is provided as negative LPT shaft offtake (in kW) to the engine model. During the hybrid run the total fuel burn and total energy are calculated. The latter is calculated by time integration of the total electric battery power in addition to the fuel burn multiplied with the fuel specific energy.

The integrated performance models were validated earlier for an A320 aircraft and a 1000 km mission with 17t payload [9][10]. The results for this mission were compared with the a/c performance simulation tool Piano-X [21] and showed good correspondence for the fuel flow prediction [12].

B. Parameter assumptions

This section describes the assumed parameter settings for MASS as applied in this paper.

1. Mission assumptions

As described above an A320neo a/c is simulated on mission of 1500 km (800 NM) with a payload of 150 passengers. A weight of 95 kg per passenger is assumed. Furthermore a fixed reserve fuel mass of ~1.8 t is assumed, accounting for alternate, contingency and reserve, estimated from [15]. This results - for this mission - in a reference a/c take-off mass of 67 t. Because the maximum take-off weight (MTOW) of the A320neo is 73.5 t [14] this leaves a “mass budget” which can be “spent” on electric components.

2. Technology level

There is a strong technology development ongoing in the field of electric components, mainly driven by other industrial sectors like automotive and consumer electronics. Because this development is expected to continue in the coming decades, several predictions of electric component technology levels can be found, e.g. see Ref.[3], Ref.[4] and Ref.[10]. In this paper we consider two technology scenarios:

⁹ In the present study power supply to the LPT shaft is considered only (HPT power supply could be considered too).

- ~2015 scenario, based on electric component technology that is available since 2015, e.g. Li-ion batteries¹⁰ or Siemens SP260D motor¹¹. This scenario is applied in comparison with the A320neo reference a/c, which entered into service in January 2016.
- ~2035 scenario, based on electric component technology level estimations, e.g. see Ref.[3], Ref.[4], and Ref.[10]. It should be noted that the uncertainty of these values is high because of the large spread in the numbers obtained from literature. This scenario is applied in comparison with the modified A320neo reference a/c: adapted to EIS in 2035.

The applied parameter values are listed in Table 5 below. Only the battery specific energy and the motor and inverter specific power values differ per scenario. The ~2035 estimates are assumed to be “conservative”. The impact of larger values will be analyzed as well, see section 3.

Table 5 Electric component parameter assumptions for the two technology levels (~2015 and ~2035) as considered in this study.

Parameter	~2015	~2035 estimate
Battery specific energy, Wh/kg	200	500
Battery efficiency, %	92.5	92.5
Battery minimum state of charge (SoC), %	10	10
Electric motor specific power, kW/kg	4	7.5
Electric motor efficiency, %	95	95
Inverter specific power, kW/kg	4	7.5
Inverter efficiency, %	95	95
Cable efficiency, %	99	99

3. Reference aircraft adaptations to EIS in 2035

In Ref.[22] and Ref.[23] examples are provided to scale an A320 to EIS in 2035. The applied modifications are listed in Table 6 below. Ref.[23] estimates a 20% reduction in specific fuel consumption (SFC) with respect to the CeRAS (IAE V2527) engine¹². In our case we assume a corresponding 20% SFC reduction with respect to the CFM-LEAP-1a26. In Ref.[23] also an engine mass of 4200 kg is applied. However, this includes the nacelle and auxiliary systems weight. The dry weight is estimated to 3000 kg, which equals more or less the dry weight of the CFM-LEAP-1a26, see Table 2. The reductions in drag coefficients are implemented as correction factors to the terms in Eq.(8). To apply the weight modifications to the reference a/c a relative structural weight breakdown of the A320 was derived from Ref.[24]. The following relevant mass percentages of the A320neo operating empty mass (mOE) were estimated:

- Fuselage: ~20% of mOE
- Wings: ~20% of mOE
- landing gear: ~ 5% of mOE
- seats: ~ 3% of mOE
- The pylons are considered part of the wing mass.

Applying these mass fractions results in an overall mOE weight reduction of 95%:

$$mOE_{2035} = mOE_{a320neo} * fact \quad (11)$$

$$fact = 0.2 * 0.9 + 0.2 * 0.95 + 0.05 * 0.85 + 0.03 * 0.4 + 0.52 * 1 = 0.95 \quad (12)$$

¹⁰ https://en.wikipedia.org/wiki/Lithium-ion_battery

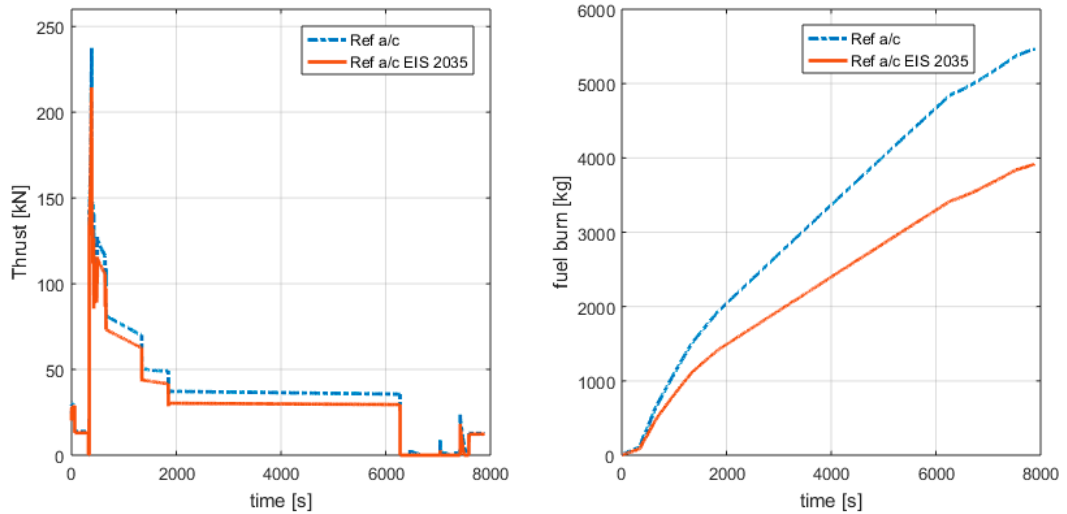
¹¹ https://en.wikipedia.org/wiki/Siemens_SP260D

¹² <http://ceras.ilr.rwth-aachen.de/trac/wiki/CeRAS/AircraftDesigns/CSR01/Propulsion%20System>

Table 6 Modifications to the A320neo a/c to obtain EIS in 2035 [22], [23].

	Modification aspect	A320 EIS in 2035	
Propulsion	SFC reduction	-20%	w.r.t. CFM-LEAP-1a26
Aero technologies (from IATA technology review)	Morphing wing	-3%	Reduction in C_d
	Turbulent coating	-5%	Reduction in $C_{d,0}$
	Shock control	-50%	Reduction in $C_{d,Mach}$
	Winglet design	-10%	Reduction in induced drag: k
Structural weight (different sources)	Wing	-10%	
	Fuselage	-5%	
	Landing gear	-15%	
	Pylons	-5%	
	Seats	-60%	

The results of performance comparison of the A320neo reference a/c and the modified EIS 2035 reference a/c - for the mission described earlier (see Fig. 3) - are depicted in Fig. 10, in terms of thrust and fuel consumption. The reductions in weight and drag result in a reduction of required thrust of $\sim 18\%$ during cruise. The overall fuel burn reduces with $\sim 30\%$. On ground the differences in performance are negligible.

**Fig. 10. Performance comparison of the A320neo reference a/c and the modified EIS 2035 reference a/c.**

III. Simulation results

A. 2015 scenario

As a first step the A320neo reference a/c was compared to a modified version with HEP, using today's level of electric component technology, see Table 5. Due to the low values for specific energy and specific power applying HEP in this scenario quickly results in drastic increases of a/c weight, exceeding the maximum take of mass (mTO_{max}). Therefore only small values for the power split ratio (ϕ) are applied during take-off and climb. Because of this small electric power supply, only very limited downscaling of the turbofan engine can be applied. Fig. 11 depicts the contours of performance results for a 98% scaled engine, with ϕ_{TO} varied between 0 and 0.15 and ϕ_{climb} varied between 0 and 0.04. The mTO_{max} value of the A320neo (73.5 t, see Table 1) is applied as constraint. Moreover the maximum value during the mission of the HPT inlet total temperature ($TT4_{max}$) is applied as constraint. A specification of $TT4_{max}$ for the CFM-Leap was not found. Therefore the $TT4_{max}$ of the reference a/c in the reference mission, which equals 1860 K, is currently used as constraint. The two constraints are depicted by red lines in Fig. 11. $TT4_{max}$ generally occurs during take-off (see Fig. 7). Therefore an increased ϕ_{TO} delivers more

power support to the LPT shaft (by the electric motor) and thereby reduces $TT4_{max}$. This does not result in reduction of fuel or energy consumption because the mOE increases due to the electric component masses. The only feasible part (satisfying the constraints $mTO < 73.5$ t and $TT4_{max} < 1860$ K) would be the small triangle in the left of the upper plots of Fig. 11, with $0.12 < \phi_{TO} < 0.13$ and $\phi_{climb} < 0.005$. But even in this area there is no advantage as the fuel and energy consumption increase with 4 to 5%.

Fig. 12 depicts the performance effects for a constant $\phi_{climb} = 0$ and with varying engine scale. In this figure it can be seen that further downscaling the engine exceeds the $TT4_{max}$ constraint of 1860 K (due to increased thermal loading of the engine). A 97% engine seems the lowest feasible reduction scale.

From this analysis it can be concluded that applying HEP on an A320 size aircraft with the current electric component technology level is feasible but does not deliver any trip fuel or –energy benefit, which is in line with previous studies [9]. This may also explain why single-aisle commercial a/c with HEP have not been developed so far.

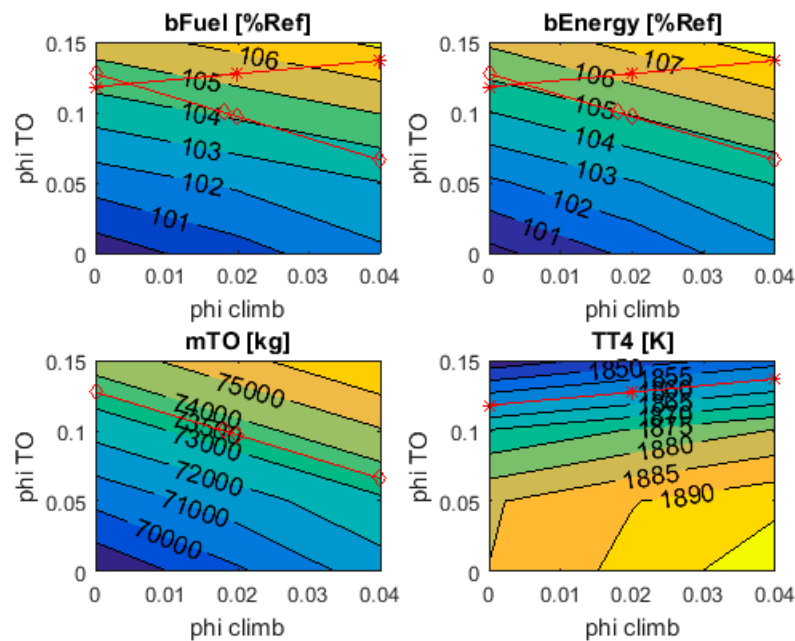


Fig. 11 HEP performance results for varied ϕ_{climb} and ϕ_{TO} , with a 98% scale engine: (upper plots) fuel and energy consumption relative to the A320neo reference a/c, and (lower plots) take-off mass (mTO) and HPT inlet total temperature TT4. The red lines depict the mTO constraint (with “diamond” markers) and TT4 constraint (with “star” markers).

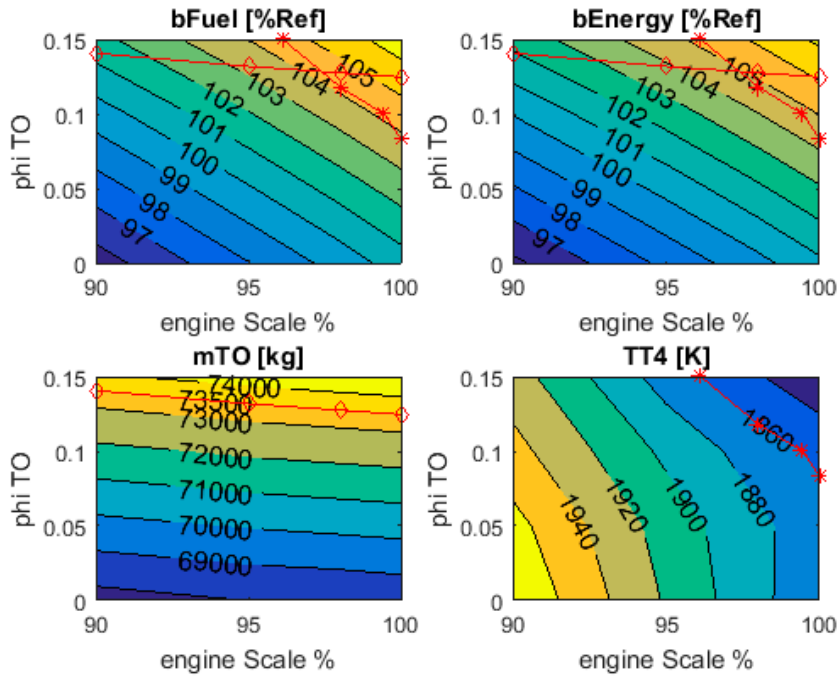


Fig. 12 HEP performance results for varied engine scale and take-off power split, with $\varphi_{\text{climb}}=0$: (upper plots) fuel and energy consumption relative to the A320neo reference a/c, and (lower plots) take-off mass (mTO) and HPT inlet total temperature TT4. The red lines depict the mTO constraint (with “diamond” markers) and TT4 constraint (with “star” markers).

B. 2035 scenario

1. Visualization of results

The A320neo reference a/c modified to EIS in 2035 (see subsection 3) was extended with HEP applying the 2035 level estimates of electric component technology, see Table 5. In this scenario HEP has more potential than in the 2015 scenario. Due to the increased specific energy and specific power values the impact of applying HEP on the a/c weight will be smaller. Moreover, the reduction in mOE (see subsection 3) and the increased performance of the EIS 2035 reference a/c (see Fig. 10) even further increase the “mass budget” for electric components as, less trip fuel is needed. The same mTO constraint (mTO < 73.5 t) is applied. The $TT4_{\text{max}}$ constraint is increased to 1900 K, which is also considered a critical temperature with respect to engine NO_x emissions [25].

Fig. 13 depicts the performance results for an 85% scale engine, with φ_{TO} and φ_{climb} varied between 0 and 0.4. From this figure it can be seen that mTO increases both with the increase of φ_{TO} and φ_{climb} due to the increased electric components mass (and trip fuel mass increase in most cases). The total energy consumption (bEnergy) - relative to the EIS2035 reference a/c total energy consumption - increases with a/c weight and therefore increases with φ_{TO} and φ_{climb} . Nevertheless a minimal value of φ_{TO} is needed in order to provide the peak power support to the downscaled engine and satisfy the $TT4_{\text{max}}$ constraint. The mass of the electric motors and power electronics is mainly impacted by φ_{TO} (taking into account the peak power during take-off) whereas the mass of the batteries is mainly impacted by φ_{climb} . Therefore the bEnergy is minimal when $\varphi_{\text{climb}}=0$, because in this case the mass of the electric components is minimized.

On the other hand increasing φ_{climb} results in a slight decrease of the fuel consumption (bFuel). Due to the increased electric power during climb less fuel is needed. However this effect is being reduced by the increased battery mass, increasing the required thrust and therefore increasing the fuel consumption, especially for larger φ_{climb} values. The minimum bFuel corresponds to a φ_{climb} value of ~ 0.2 .

Similar to the previous subsection the HEP performance results are also depicted for a varying engine scale, see Fig. 14, with $\varphi_{\text{climb}}=0$. This figure shows that an engine scale smaller than 82% is unfeasible due to the $TT4_{\text{max}}$ constraint. Furthermore this figure shows that a minimum energy consumption can be achieved with a $\sim 85\%$ scaled engine, although the differences in terms of energy consumption with respect to the other engine scales are small. Generally a 5% reduction in energy consumption can be achieved with the engine scales between 82% and 90%.

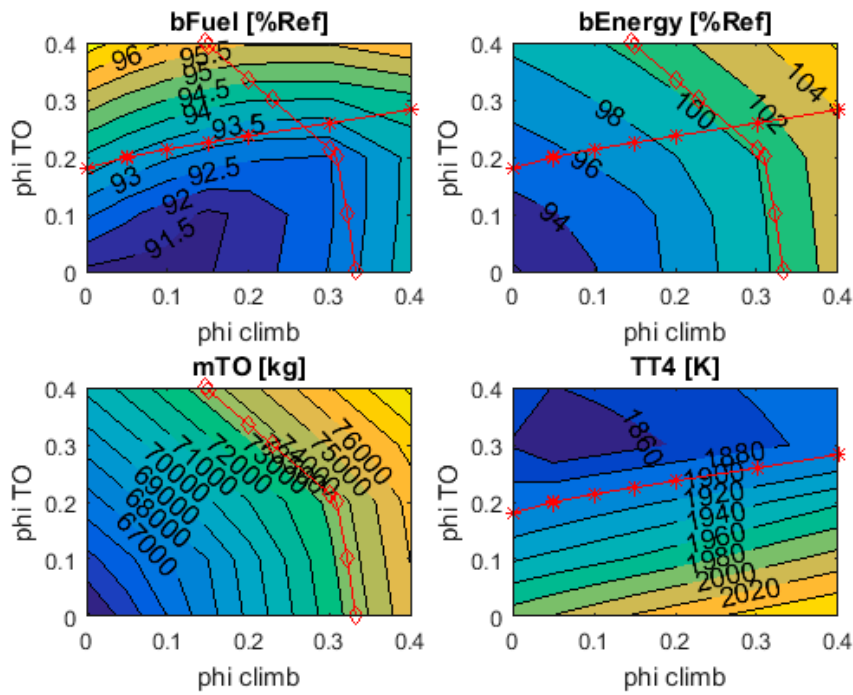


Fig. 13 HEP performance results for varied ϕ_{climb} and ϕ_{TO} , with an 85% scale engine: (upper plots) fuel and energy consumption relative to the EIS2035 reference a/c, and (lower plots) take-off mass (mTO) and HPT inlet total temperature TT4. The red lines depict the constraints: mTO (with “diamond” markers) and TT4 (with “star” markers).

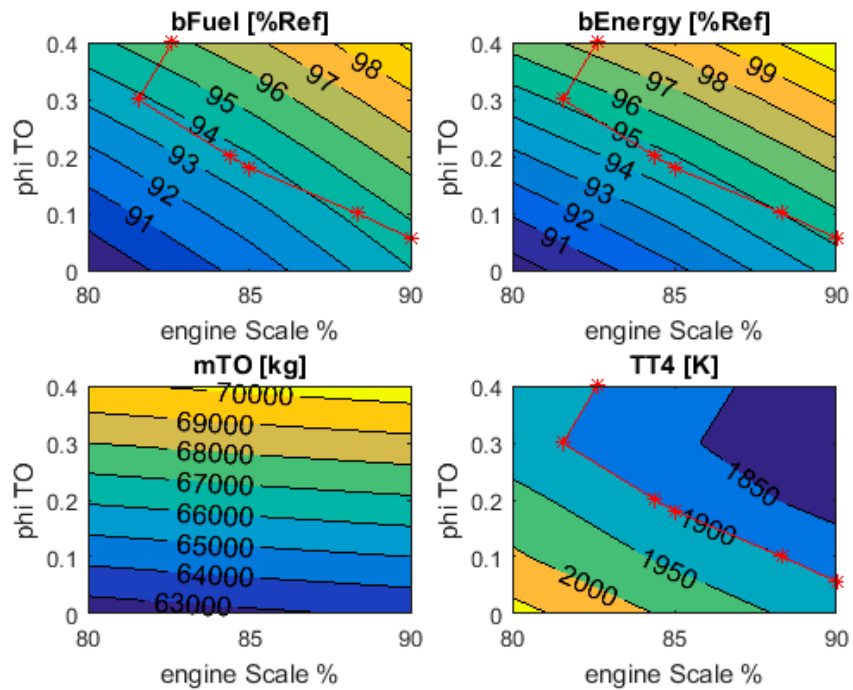


Fig. 14 HEP performance results for varied engine scale and ϕ_{TO} , with $\phi_{climb}=0$: (upper plots) fuel and energy consumption relative to the EIS2035 reference a/c, and (lower plots) take-off mass (mTO) and HPT inlet total temperature TT4. The red line depicts the TT4 constraint (with “star” markers).

Besides fuel burn and energy consumption also the engine emissions can be considered as optimization objective. Fig. 15 shows that downscaling the turbofan engine decreases the emission of CO₂ (which directly relates to fuel burn), CO and UHC but increases the NO_x emission due to the TT4_{max} constraint. To avoid NO_x emissions worse than the reference a/c the 90% scaled engine seems a better compromise than for example the 85% scaled engine. In Fig. 16 both the fuel and energy consumption and corresponding emissions are shown. This figure shows that the optimal performance can be found with a $\phi_{climb} < 0.15$ and $0.05 < \phi_{TO} < 0.1$, depending on what performance criterion is emphasized more (fuel, energy or NO_x emission).

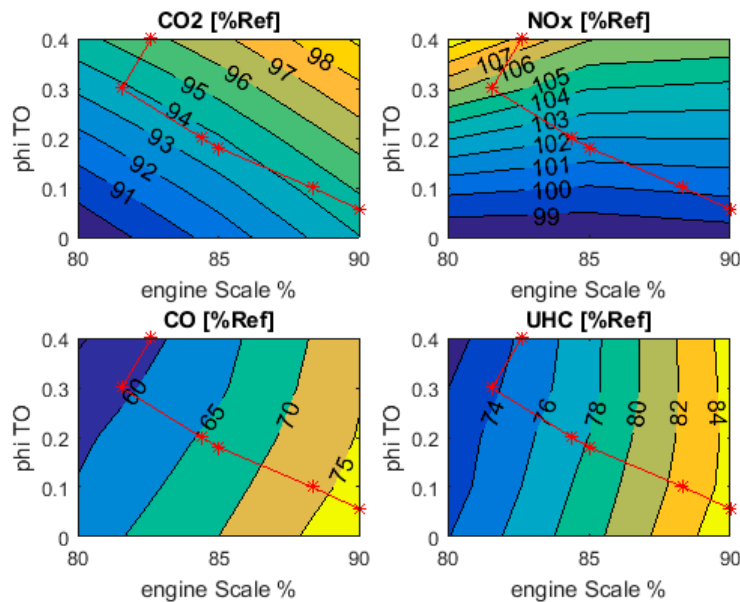


Fig. 15 HEP emission predictions relative to the EIS2035 reference a/c for varied engine scale and ϕ_{TO} , with $\phi_{climb}=0$: (upper plots) CO₂ and NO_x, and (lower plots) CO and UHC. The red line depicts the TT4 constraint (with “star” markers).

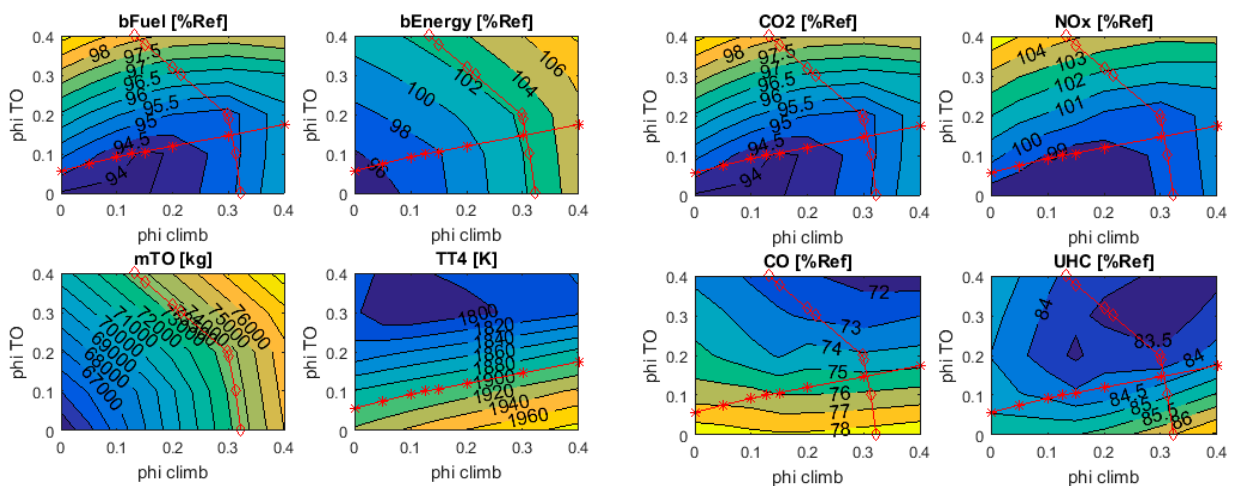


Fig. 16 HEP performance and emission predictions for varied ϕ_{climb} and ϕ_{TO} , with a 90% scale engine: (upper plots) fuel and energy consumption and CO₂ and NO_x relative to the EIS2035 reference a/c, and (lower plots) mTO and TT4, and CO and UHC. The red lines depict the mTO constraint (with “diamond” markers) and TT4 constraint (with “star” markers).

2. Optimization of results

The optimal φ_{climb} , φ_{TO} , and engine scale can also be derived using a mathematical optimization approach. The optimization problem is formulated as follows:

$$\begin{aligned} & \min_x f(x) \\ & \text{subject to: } g(x) \leq 0 \\ & \text{bounded by: } x_{lb} \leq x \leq x_{ub} \end{aligned} \quad (13)$$

In Eq.(13) above

- the “design” vector $x := (\varphi_{climb}, \varphi_{TO}, \text{engine scale})$ representing a three-dimensional design space;
- the lower and upper bounds x_{lb} and x_{ub} are (0, 0, 80%) and (0.4, 0.4, 90%) , respectively, in correspondence with the axes of previous contour plots;
- the objective function $f(x)$ can either be fuel burn, energy consumption or NO_x emission;
- the constraint function $g(x)$ is two-dimensional:

$$g(x) = \begin{pmatrix} TT4_{max}(x) - 1900 \\ mTO(x) - 73500 \end{pmatrix} \quad (14)$$

The fuel, energy and NO_x optimizations were performed using a sequential quadratic programming (SQP) algorithm (gradient method), provided by the MATLAB service *fmincon*⁴. Each evaluation of $f(x)$ or $g(x)$ requires a complete simulation run of the hybrid a/c configuration. In order to improve the efficiency of the optimization process a surrogate model was derived for f and g . The data set of simulation results with variation of φ_{climb} , φ_{TO} , and engine scale between x_{lb} and x_{ub} - that was visualized in previous contour plots - was interpolated, using NLR’s MultiFit tool [26]. A kriging interpolation method [26] with quadratic regression function and exponential correlation function was applied. The optimization results are listed in Table 7 below. The optimization was performed using the kriging interpolation functions (kri). After that the simulation run of hybrid a/c configuration was carried out again with the derived optimal “design” vector $x_{opt} = (\varphi_{climb}, \varphi_{TO}, \text{engine scale})$ as parameter settings. The resulting fuel burn, energy consumption and NO_x emission are added to the table as well, as “validation” values (val). The “validation” values have a negligible deviation from the kriging interpolation predictions.

Table 7 Optimization results with respect to fuel burn (first row), energy consumption (second row), and NO_x emission (third row). In each case the result by interpolation (kri), validation with original simulation (val), and percentage of the reference a/c value (%Ref) is given.

Design variables			Objectives								
φ_{climb}	φ_{TO}	%Engine	bFuel kg kri	bFuel kg val	%Ref	bEnergy MWh kri	bEnergy MWh val	%Ref	NO_x g kri	NO_x g, val	%Ref
0.149	0.166	86.7	3643.6	3644.3	93.1	45.49	45.50	97.2	38.0	38.12	99.5
0.000	0.153	85.4	3658.3	3659.3	93.5	44.15	44.16	94.4	38.6	38.69	101.0
0.150	0.104	90.0	3677.5	3677.7	93.9	45.82	45.82	97.9	37.7	37.73	98.5

3. Trend analysis of technology parameter assumptions

The optimization approach described in previous subsection was extended by repeating it sequentially for varied settings of specific energy (sE) and specific power (sP). In this way it is investigated what minimal fuel and energy can be achieved, for a specific setting of the battery sE and the sP of the electric motors and inverters. The ~2035 estimates as stated in Table 5 are considered “conservative”. Therefore the battery sE was varied between 500 and 1000 Wh/kg, and the sP (with the same value for the electric motors and inverters) was varied between 7.5 and 15 kW/kg. For each combination of sE and sP

- φ_{climb} was varied with steps of 0.2 between 0 and 0.8;
- φ_{TO} was varied with steps of 0.2 between 0 and 0.6;
- the engine scale was varied between 80% and 90%;
- a kriging interpolation was applied to the data set of simulation results;
- the same optimization problem as formulated in Eq.(13) was solved using SQP.

The results in terms of minimal fuel burn and minimal energy consumption are visualized by the contour plots in Fig. 17. Furthermore the corresponding optimal settings in terms of φ_{climb} , φ_{TO} and engine scale, and the corresponding values of m_{TO} and TT4_{max} are listed in Table 8 (for the fuel based optimizations) and Table 9 (for the energy based optimizations). The optimization results in the first row of Table 8 and Table 9 differ from the results in Table 7 because now a coarser grid of variations was used (steps of 0.2 in φ_{climb} , and φ_{TO} , instead of 0.1) resulting in different interpolations.

In Fig. 17 it can be seen that the minimal fuel burn is mostly impacted by the change in sE. This change directly relates to the achievable battery mass which on its turn allows for fuel reduction (compensated to some extent by additional fuel needed for the increase in mOE). The minimal energy consumption is both impacted by the sE and sP. In general the impact of sE and sP on the minimal energy consumption is small: only a reduction of a few percent more can be achieved when doubling sE and sP. The main reason is that the reduction in energy needs to come from the engine downscaling. However it turns out that an engine scale below 82% does not satisfy the constraint of $\text{TT4}_{\text{max}} < 1900$ K. This was already shown in Fig. 14 and it also follows from the derived optimal settings in the sequential runs, Table 8 see and Table 9. The minimal fuel burn can be reduced a bit more, because this criterion depends on the battery mass and therefore takes advantage of the increases in specific energy.

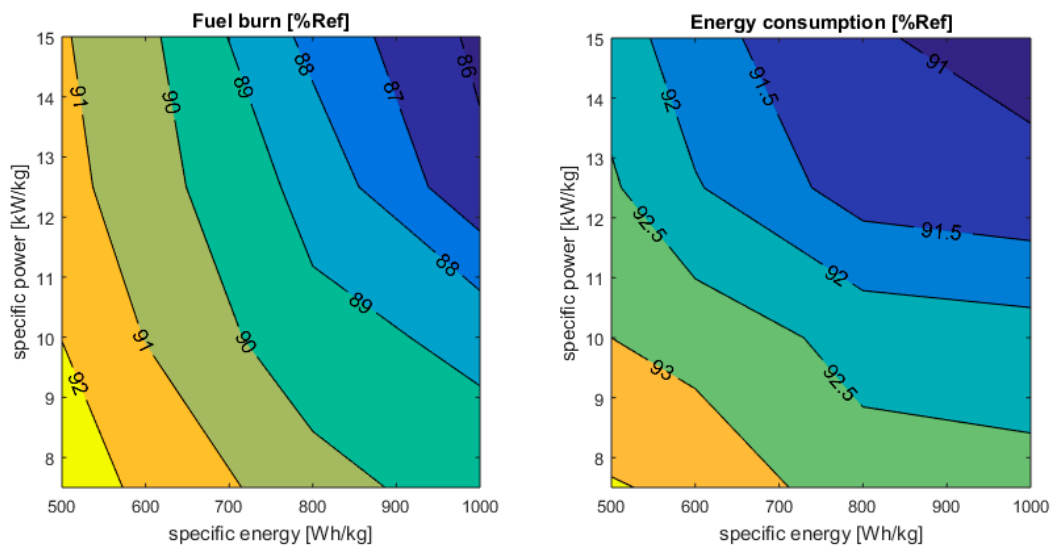


Fig. 17. Contour of minimal fuel burn (left) and minimal energy consumption (right), both as percentage of the EIS2035 reference a/c, and as function of specific energy and power assumptions of electric components.

Table 8 Specific energy and power impact on minimized fuel burn, with corresponding optimum settings of φ_{climb} , φ_{TO} , and engine scale.

Specific energy Wh/kg	Specific power kW/kg	φ_{climb}	φ_{TO}	%Engine	mTO kg	TT4max K	Fuel burn kg	Fuel burn %Ref
500	7.5	0.04	0.14	84.8	66354	1900	3623.6	92.6
500	10	0.04	0.15	84.3	65897	1900	3601	92.0
500	12.5	0.03	0.16	83.8	65248	1900	3575.5	91.3
500	15	0.20	0.17	85.2	69248	1900	3566.3	91.1
600	7.5	0.20	0.16	85.8	69731	1900	3593.3	91.8
600	10	0.20	0.17	85.4	68996	1900	3561	91.0
600	12.5	0.04	0.25	81.9	66042	1900	3540.1	90.4
600	15	0.05	0.17	82.9	65102	1900	3532.2	90.2
800	7.5	0.20	0.16	85.2	68473	1900	3539.6	90.4
800	10	0.40	0.18	86.3	71435	1900	3495.9	89.3
800	12.5	0.20	0.18	83.6	67344	1899.9	3471	88.7
800	15	0.40	0.18	84.8	70382	1900	3433.7	87.7
1000	7.5	0.20	0.17	84.6	67744	1900	3501.9	89.5
1000	10	0.20	0.17	84.5	67070	1899.9	3475.6	88.8
1000	12.5	0.40	0.25	83.0	69746	1900	3376.8	86.3
1000	15	0.40	0.25	82.8	69324	1900	3357.8	85.8

Table 9 Specific energy and power impact on minimized energy consumption, with corresponding optimum settings of φ_{climb} , φ_{TO} , and engine scale.

Specific energy Wh/kg	Specific power kW/kg	φ_{climb}	φ_{TO}	%Engine	mTO kg	TT4max K	Energy consumption MWh	Energy consumption %Ref
500	7.5	0.00	0.12	85.0	64944	1900	43.8	93.5
500	10	0.00	0.14	84.2	64664	1900	43.5	93.0
500	12.5	0.01	0.15	83.8	64664	1900	43.3	92.6
500	15	0.00	0.15	83.3	64307	1900	43.2	92.3
600	7.5	0.00	0.12	84.8	64797	1900	43.7	93.4
600	10	0.00	0.14	84.0	64560	1900	43.4	92.8
600	12.5	0.01	0.15	83.6	64618	1900	43.1	92.0
600	15	0.01	0.17	82.7	64357	1900	42.9	91.7
800	7.5	0.02	0.14	84.3	65096	1900	43.4	92.7
800	10	0.02	0.15	83.8	64749	1900	43.2	92.3
800	12.5	0.01	0.17	82.3	64457	1900	42.7	91.3
800	15	0.01	0.18	82.2	64222	1900	42.6	91.0
1000	7.5	0.02	0.14	83.9	65137	1900	43.4	92.7
1000	10	0.02	0.15	83.7	64659	1900	43.2	92.2
1000	12.5	0.01	0.17	82.3	64317	1900	42.6	91.1
1000	15	0.01	0.18	82.1	64074	1900	42.5	90.9

IV. Conclusions and perspectives

A parametric system model and tool chain implementation has been developed, called MASS: Mission, Aircraft and Systems Simulation for HEP performance analysis. MASS simulates the performance of a specified aircraft configuration, including engines and electric systems, for a given mission. The fuel flow and electric power are calculated as function of time in order to predict the total energy consumption. Furthermore the engine emissions are calculated.

First an Airbus A320neo reference aircraft with 150 passengers on a 1500 km (800 NM) mission was compared to a modified version with a parallel HEP architecture to electrically support the turbofan engine during take-off and climb phases. From this analysis it can be concluded that applying HEP on an A320 size aircraft with the electric component technology level of today is feasible but does not deliver any trip fuel or –energy benefit, due to the drastic increase of system weight, which is in line with previous studies [7].

Second an “upgraded” version of the A320neo reference a/c - modified to EIS in 2035 – was compared to its hybrid counterpart, applying the same mission and the same parallel HEP architecture as before but now with electric component technology estimations for 2035. In this case reductions of fuel and total energy consumption up to 7% and 5 % respectively, can be achieved, depending on the power split settings during take-off and climb. The reductions in fuel and energy consumption are achieved by downscaling the engine - which results in a lower engine mass and a better performance during cruise - and supporting the take-off phase by providing additional power to the LPT shaft using electric motors. The fuel consumption (contrary to the total energy consumption) can be further reduced by providing electric power for a longer period during the climb phase. Too much electric energy during climb reverses this fuel reduction though, due to the increase in system mass caused by the required batteries. Optimal settings for the take-off and climb power split were found depending on which performance criterion is emphasized more.

Furthermore, it was found that engine emissions in terms of CO and UHC are reduced with the fuel and energy optimization but NO_x emissions may increase, due to the higher temperatures that come with engine downscaling. Apart from individual optimizations of fuel burn, energy consumption, and NO_x emission also a compromised optimum was found for a 90% scaled engine resulting in 6% fuel reduction, 2% energy reduction and 1.5% NO_x reduction.

From the additional trend analysis of varying the specific energy and specific power assumptions of the electric components, it can be concluded that the impact of this variation on the minimized energy consumption is small: only a few percent further reduction can be achieved when doubling specific energy and power. The main reason is that the reduction in energy needs to come from the engine downscaling which is restricted by the maximum HPT inlet temperature. The minimal fuel burn can be reduced a bit more, because this criterion also depends on the battery mass and therefore takes advantage of the increases in specific energy.

The current restrictions in downscaling of the turbofan engine could be mitigated by reducing the required thrust per engine. If part of the a/c thrust requirement is divided over electrically driven propulsors parallel to the turbofan engines, the thrust to be delivered by the turbofans is reduced. As such, it is expected that the turbofan engine temperatures decrease, enlarging the potential for engine downscaling. Analyzing such parallel HEP configurations with MASS will be part of further work.

Other items for further research are the application of electric power during flight phases other than take-off and climb (e.g. descent, taxi) and the potential of generation of electric energy during cruise, to re-charge the batteries in-flight for deployment during descent and taxi-in. This could lead to a further optimized power management in relation to the a/c mission that needs to be performed. In addition, specific optimizations of the missions for HEP aircraft, for example in terms of range, payload, speed and altitude are of interest.

Acknowledgments

This work has received funding from the Clean Sky 2 Joint Undertaking under the European Union’s Horizon 2020 research and innovation program under grant agreement CS2-LPA-GAM-2018/2019-01. The authors would like to thank the other Clean Sky 2 partners (Airbus, Rolls-Royce, DLR, ONERA and TU Delft) involved in this work for the valuable discussions and technical exchanges.

References

- [1] Airbus, 2019, “Global market forecast 2019-2038”, <https://www.airbus.com/aircraft/market/global-market-forecast.html>. [retrieved on 26 November 2019]
- [2] European Commission, “Flightpath 2050 Europe’s Vision for Aviation, Report of the High Level Group on Aviation Research”, ISBN 978-92-79-19724-6, European Union, 2011. doi 10.2777/50266.

- [3] Brelje, B. J., and Martins J. R. R. A., “Electric, Hybrid, and Turboelectric Fixed-Wing Aircraft: A Review of Concepts, Models, and Design Approaches”, *Progress in Aerospace Sciences*, Vol. 104, 2019, pp. 1-19, ISSN 0376-0421. doi:10.1016/j.paerosci.2018.06.004
- [4] National Academies of Sciences (NAS), Engineering, and Medicine, *Commercial Aircraft Propulsion and Energy Systems Research: Reducing Global Carbon Emissions*, The National Academies Press, 2016. doi 10.17226/23490.
- [5] Felder J. L., NASA Glenn Research Center, “NASA Hybrid Electric Propulsion Systems Structures,” presentation to the committee on September 1, 2015.
- [6] European Union Clean Sky 2 (EU CS2), Large Passenger Aircraft (LPA), <https://www.cleansky.eu/large-passenger-aircraft>, [retrieved on 11 June 2019].
- [7] De Vries, R., Hoogreef, M. F. M., and Vos, R., “Preliminary Sizing of a Hybrid-Electric Passenger Aircraft Featuring Over-the-Wing Distributed-Propulsion,” *AIAA Scitech 2019 Forum*, 2019, p. 1811.
- [8] Hoogreef, M. F. M., Vos, R., de Vries, R., and Veldhuis, L. L., “Conceptual Assessment of Hybrid Electric Aircraft with Distributed Propulsion and Boosted Turbofans,” *AIAA Scitech 2019 Forum*, 2019, p. 1807.
- [9] Ang, A. W. X., Gangoli Rao, A., Kanakis, A., and Lammen, W. F., “Performance analysis of an electrically assisted propulsion system for a short-range civil aircraft,” *Journal of Aerospace Engineering*, Vol. 233 No. 4, Feb 2018, pp. 1490-1502, NLR-TP-2018-019.
- [10] Tan, S. C., “Electrically Assisted Propulsion & Power Systems for Short-Range Missions: Electrification of a Conventional Airbus A320neo”, MSc. Thesis TU Delft, April 2018.
- [11] Lammen, W., and Vankan, J., “Electrification studies of single aisle aircraft: a ‘retrofit’ investigation including parallel hybrid electric propulsion”, *International Symposium on Sustainable Aviation (ISSA-2019)*, Budapest, Hungary, 26-29 May 2019, NLR-TP-2019-312.
- [12] Vankan, J., and Lammen, W., “Parallel hybrid electric propulsion architecture for single aisle aircraft - powertrain investigation”, *9th EASN International Conference on “Innovation in Aviation & Space”*, Athens, Greece, 3-6 September, 2019, NLR-TP-2019-358.
- [13] Airbus Customer Services, 2002, *Getting to Grips with Aircraft Performance*, <https://www.skybrary.aero/bookshelf/books/2263.pdf> [retrieved on 26 November 2019].
- [14] European Aviation Safety Agency (EASA), Type-Certificate Data Sheet No. EASA.A.064: Airbus A318 - A319 - A320 - A321, 2018.
- [15] International Civil Aviation Organization (ICAO), Annex 6 Operation of Aircraft – Part 1: International Commercial Air Transport – Aeroplanes, 2010.
- [16] European Aviation Safety Agency (EASA), Type-Certificate Data Sheet: No. E .110 for Engine LEAP-1A & LEAP-1 C series engines, 2018.
- [17] Chakraborty, I., Mavris, D. N., and Emeneth, M., “Methodology for Vehicle and Mission Level Comparison of More Electric Aircraft Subsystem Solutions - Application to the Flight Control Actuation System”, *Journal of Aerospace Engineering*, Vol. 229, pp. 1088-1102, 2015.
- [18] Chakraborty, I., Mavris, D. N., Emeneth, M., and Schneegans, A., “An Integrated Approach to Vehicle and Subsystem Sizing and Analysis for Novel Subsystem Architectures”, *Journal of Aerospace Engineering*, Vol. 230, pp. 496–514, 2016.
- [19] Scholz, D., Seresinhe, R., Staack, I., and Lawson, C., “Fuel Consumption due to Shaft Power Off-Takes from the Engine”, *4th International Workshop on Aircraft System Technologies*, AST 2013.
- [20] International Civil Aviation Organization, “ICAO Aircraft Engine Emissions Databank,” Tech. Rep., 2019. <https://www.easa.europa.eu/easa-and-you/environment/icao-aircraft-engine-emissions-databank>, [retrieved on 20 November 2019].
- [21] Simos, D., Piano-X, 2017.
- [22] Schmollgruber, P., Döll, C., Hermetz, J., Liaboeuf, R., Ridet, M., et al., “Multi- disciplinary Exploration of DRAGON: an ONERA Hybrid Electric Distributed Propulsion Concept” *AIAA Scitech 2019 Forum*, Jan 2019, SAN DIEGO, United States. hal-02068597.
- [23] Schmollgruber, P., et al., Multidisciplinary Design and performance of the ONERA Hybrid Electric Distributed Propulsion concept (DRAGON), *AIAA Scitech 2020*, submitted for publication.
- [24] De Marco, A., Nicolosi, F., Attanasio, L., and Vecchia, P., “A Java desktop application for Aircraft Preliminary Design”, *Second International Conference On Advances in Information Processing and Communication Technology - IPCT 2015*. doi 10.15224/978-1-63248-044-6-20.
- [25] Lefebvre, A. H., and Dilip, R.B., *Gas Turbine Combustion: Alternative Fuels and Emissions*, Taylor and Francis Group, United States, third edition, 2010. ISBN 978-1-4200-8605-8.
- [26] Vankan, W. J., Lammen, W. F., and Maas, R., “Meta-modeling and multi-objective optimization in aircraft Design”, Editors E. Kesseler, and M.D. Guenov; *Advances in collaborative civil aeronautical multidisciplinary design optimization. Progress in Astronautics and Aeronautics*; Vol. 233; American Institute of Aeronautics and Astronautics, Reston, VA, chapter 6, 2010.



Dedicated to innovation in aerospace

Royal Netherlands Aerospace Centre

NLR is a leading international research centre for aerospace. Bolstered by its multidisciplinary expertise and unrivalled research facilities, NLR provides innovative and integral solutions for the complex challenges in the aerospace sector.

NLR's activities span the full spectrum of Research Development Test & Evaluation (RDT & E). Given NLR's specialist knowledge and facilities, companies turn to NLR for validation, verification, qualification, simulation and evaluation. NLR thereby bridges the gap between research and practical applications, while working for both government and industry at home and abroad.

NLR stands for practical and innovative solutions, technical expertise and a long-term design vision. This allows NLR's cutting edge technology to find its way into successful aerospace programs of OEMs, including Airbus, Embraer and Pilatus. NLR contributes to (military) programs, such as ESA's IXV re-entry vehicle, the F-35, the Apache helicopter, and European programs, including SESAR and Clean Sky 2. Founded in 1919, and employing some 600 people, NLR achieved a turnover of 76 million euros in 2017, of which 81% derived from contract research, and the remaining from government funds.

For more information visit: www.nlr.org

Postal address

PO Box 90502
1006 BM Amsterdam, The Netherlands
e) info@nlr.nl | www.nlr.org

NLR Amsterdam

Anthony Fokkerweg 2
1059 CM Amsterdam, The Netherlands
p) +31 88 511 3113

NLR Marknesse

Voorsterweg 31
8316 PR Marknesse, The Netherlands
p) +31 88 511 4444